Study within the Mining Effects Knowledge Program (KEM-39) on the cyclic storage of gases in the Netherlands

WP2 - ANALYSIS OF LABORATORY TESTS: MECHANICAL WEAKENING AND DAMAGE OF THE RESERVOIR ROCK AND CAPROCK INDUCED BY CO2, H2, N2 EFFECTS

Authors:
Eng. Isotton Giovanni[1]
Prof. Janna Carlo[1]
Prof. Teatini Pietro[1]
Prof. Deangeli Chiara[2]
Prof. Rocca Vera[2]
Prof. Verga Francesca[2]
Prof. Collettini Cristiano[3]

Affiliations:
[1]M3E srl
[2]Politecnico di Torino
[3]Università la Sapienza

Document type: Technical report

Date: December 2022

INDEX

1 Intro....3

2 Analysis of laboratory tests....3

2.1 Conclusion 32

3 Advances of research on H2 storage 33

References....36

1 Intro

Depleted oil and gas fields are good targets for gas storage both in offshore and onshore environments. Changes in the properties of the reservoir rocks, due to gas–brine–rock interaction, can affect performance, efficiency and safety of the storage process. Consequently, the effect of gas –brine on the mineralogical, petrophysical and geomechanical properties of reservoir rocks must be addressed (Peter et al., 2022).

This WP reports the results of studies focused on laboratory tests carried out on rock specimens for the evaluation of the changes in mechanical properties of the rock with different gases: CO2, H2, N2.

The injection and storage of CO2 has been working safely and effectively over several decades around the world. Over 40 sites have or are presently injecting over 200 million tonnes of anthropogenic CO2.

Consequently, the majority of experiments reported in the literature mainly refer to CO2 injection in rock specimens. The mechanical response of rock injected with N2 is marginally investigated. Likewise, lab tests for the analysis of the mechanical behavior of rock with H2 injection are developing.

2 Analysis of laboratory tests

The injection of CO2 in deep geological formations induces geochemical disequilibrium from mixing of CO2 and resident brine (Espinoza et al., 2018), leading to reactions with minerals in the host rock, including potential mineral dissolution/precipitation and clay fabric alteration (Gunter et al., 2000; Kaszuba et al., 2005; McGrail et al., 2009; Espinoza and Santamarina, 2012; Yoksoulian et al., 2013). These chemical reactions may occur in the reservoir/storage rock, the caprock, well-cement interfaces, and in fault gouge material, if contacted by CO2 (Espinoza et al., 2018).

As injection goes on, the reservoir area around the injection well is expected to present different zones according to the saturation state. Close to the well, the pore fluid should be exclusively gaseous CO2. The (quasi-) fully saturation by scCO2, induces the drying effect and may lead to salt precipitation. As one moves away from the well, a mixture of scCO2 and acidified brine (two phase mixture) would then be gradually encountered (Bemer & Lombard, 2010), with expected buffered pH as outlined by Gaus (2010). Even farther, the host rock should be saturated with an acidified

aqueous CO2 solution, before reaching a remote unaffected zone (André et al., 2007). Once present in the reservoir, CO2 may enter the cap rock in gaseous state if the gas pressure exceeds the cap rock entry pressure or in dissolved state through diffusion processes. Figure 1 shows the zones affected by different gas saturation spatial distribution.

Peter et al. (2022) indicated that any change in a property will affect a chain of other properties. ~~As,~~ The pressure and temperature conditions of the reservoir are dynamic, and the salinity of brine can change depending on the amount of dilution at any given time. This means that the flow properties of CO2–brine in reservoir rock will change over time. Ilgen et al. (2018) and Rutqvist (2012) showed that chemical and mechanical changes in the properties of reservoir rocks are coupled. Therefore, a change in the chemical composition of the rocks by dissolution, precipitation, or pore stress corrosion will lead to a change in strength and deformability properties of the rocks. Once CO2 is injected into a reservoir for storage, it mixes with the fluid in the reservoir, and the properties of CO2, brine, and the reservoir change over time. Furthermore, the density of CO2-bearing brine is higher than brine; thus, CO2-saturated brine sinks to the bottom. This process of density settling creates hydrodynamic processes that are necessary for CO2–brine mixing and dissolution. The undissolved CO2 is lighter and rises to the top of the mix by buoyancy.

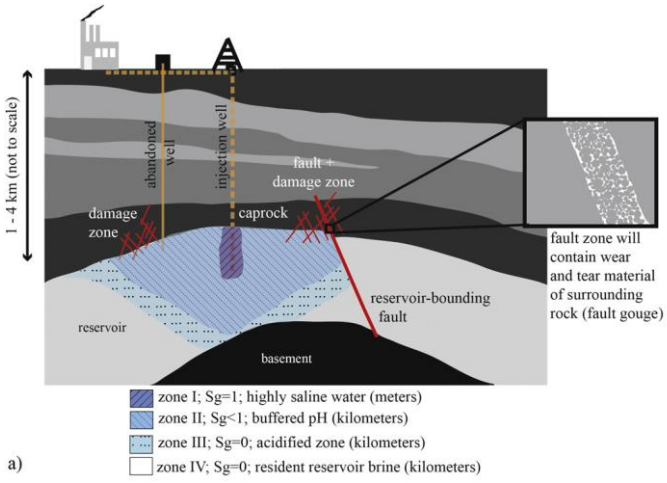

Figure 1. Schematic overview of the storage complex with different zones around the injection well depending on the spatial distribution of CO2 saturation (Rohmler et al., 2016).

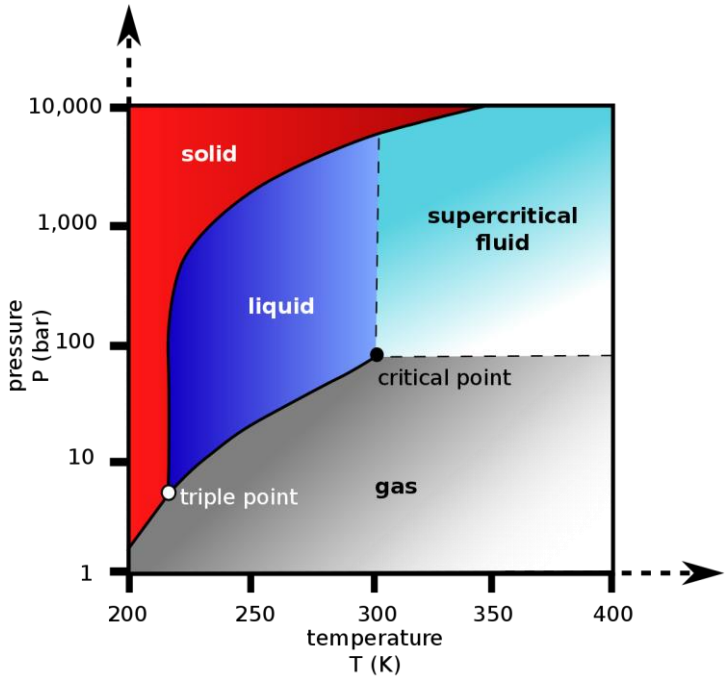

Figure 2. State diagram of CO2.

Several geochemical and geomechanical investigations of the fluid-CO2-rock interaction have been carried out on sedimentary rocks (sandstone, carbonate, shale and anhydrite). Supercritical CO2 is the most popular phase of CO2 that has been used in geological storage research. This is because CO2 is injected in supercritical conditions into the reservoir. Peter et al. (2022) indicated that once CO2 is injected in supercritical conditions into the reservoir the dynamic pressure-temperature condition of the reservoir, induces the change of phase of CO2. This effect therefore needs the investigation of the impact of other phases of CO2 in geological CO2 storage. Figure 2 shows the state diagram of CO2.

A thorough review of CO2- fluid-rock interactions was presented by Rohmer et al. (2016) and Peter et al. (2022). They summarized a large set of laboratory experiments setup for the analysis of geochemical and geomechanical changes of the rock properties.

The results of the experiments indicate that the injected CO2 is prone to dissolve within the resident reservoir pore fluid (Rohmer et al., 2016). The solubility reaction of CO2 in brine is highly sensitive to temperature and pressure and to the salt concentration of the brine (Rathnaweera et al. 2015). Injected CO2 dissolves as carbonic acid, causing a drop in pH of the brine to 4-5. The pH drop promotes dissolution of numerous minerals and in some cases results in secondary mineral precipitation (Fuchs et al., 2019). The interactions with carbonate minerals results in buffering the

pH and ultimately make the brine less acidic. This is followed by slower reactions with silicate and phyllosilicate minerals that further raise the pH, and cause precipitation of clays and carbonates in the more distant regions (Kampman et al., 2014; Shi et al., 2019).

Pore-network of the reservoir rock is significantly affected by dissolution and precipitations of the minerals, which consequently changes the permeability of the porous medium. Porosity and permeability can potentially increase, due to initial dissolution of carbonates and clay minerals, but secondary precipitation of these mineral can decrease porosity and might decrease permeability. Matter et al., 2016 observed that secondary precipitation may occur, but only after long time periods, and only when the pH reaches a (relatively) high number again.

Bolourinejad et al. (2014) and Bolourinejad (2015) carried out laboratory experiments with scCO2 flooding on core samples from Rotliegend sandstone reservoir and Zechstein anhydrite and carbonate caprock from a selection of gas fields in northeast Netherlands. The average mineralogy of Rotliegend reservoir sandstone (8 samples) and Zechstein caprock (5 samples) is reported in Figure 3.

Mineral	Reservoir samples	Caprock samples	
		Anhydrite layer	Carbonate layer
Quartz	90 %	0%	2.5%
Albite	5 %	0%	0%
K-feldspar	2%	0%	0%
Kaolinite	1.5%	0%	0%
Dolomite	<1%	12.5%	21.5%
Illite	<1%	0%	0%
Anhydrite	<1%	87.5%	8.5%
Halite	<1%	0%	3.5%
Calcite	0%	0%	64%

Figure 3. Mineralogy (weight percentage) of Rotliegend reservoir sandstone and Zechstein caprock in the Northeast Netherlands (Bolourinejad, 2015).

Figure 4 shows the initial porosity and permeability of the reservoir rock. The rock samples were subjected to in situ conditions (300 bar, 100°C) with presence of brine (pH=6.8), methane (2%) and scCO2. The duration of the tests was 30 and 143 days. After injection of CO2, the processes of dissolution promoted a drop in pH of the brine pH=6.1. On the other hand, the results of simulations carried out with TOUGHREACT software indicated pH=4.3 (Bolourinejad et al., 2014).

In general, the experimental results are expected to be more reliable, although some inaccuracies can occur. The results of the study of Bolourinejad (2015) indicates that the prediction of pH reduction with modeling software can overestimate the drop of pH of the brine after CO2 exposure. This outcome could suggest that also a detailed analysis of the composition of the brine is necessary. In the reservoir samples quartz, albite, k-feldspar and kaolinite dissolution occurred after 30 days of experiment due to the formation of carbonic acid. Furthermore, fresh precipitation of kaolinite, associated with the dissolution of albite, was observed in the samples after CO2 injection. In addition, the precipitation of dawsonite in reservoir samples was observed in a long term (143 days). In the caprock samples anhydrite, dolomite and calcite dissolution were observed due to the formation of carbonic acid.

The magnitude of minerals dissolution/ precipitation in the reservoir samples, was estimated with the change of permeability before and after the experiments. After 30 days of CO2, brine and rock interaction, the permeability of the samples increased in all cases due to the dominance of mineral dissolution over precipitation. Permeability increased by 10 to 30% (i.e. by a factor of 1.1 to 1.3) except in one case where permeability increased by a factor of 5.

In the caprock the permeability increased by a factor of 3 to 10 due to the mineral dissolution. Bolourinejad (2015) observed that the measured reactive surface areas were significantly higher than what is typically being used in modeling studies (e.g. Xu et al., 2007), which leads to more dissolution / precipitation of minerals.

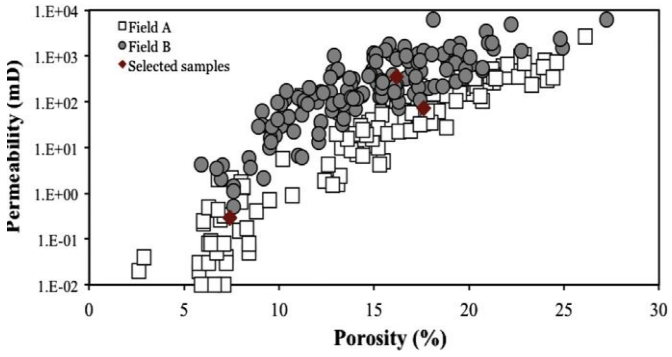

Figure 4. Initial porosity and permeability of the reservoir rock in the Northeast Netherlands (Bolourinejad & Herber, 2015).

The comparison between experiments and modeling results shows some deviations related to the magnitude and time scale of changes in mineral dissolution and precipitation. This outcome indicates that the variables of the geochemical system are difficult to be characterized.

Furthermore, Bolourinejad & Herber (2015) investigated the effect of sulfur dioxide injection with carbon dioxide on the mineralogy and permeability of Rotliegend reservoir rock and Zechstein caprock from gas fields in northeast Netherlands. They found that after the experiments the permeability of the reservoir samples had increased by a factor of 1.2–2.2 as a result of dissolution of primary reservoir minerals. Analysis of the associated brine samples before and after the experiments showed that concentrations of K, Si and Al had increased, indicative of silicate mineral dissolution.

In the caprock samples, composed of carbonate and anhydrite minerals, permeability changed by a factor of 0.79–23. The increase in permeability is proportional to the amount of carbonate in the caprock. With higher carbonate content in comparison with anhydrite the permeability increase is higher due to the additional carbonate dissolution.

Based on the results of tests carried out on Rotliegend sandstones of the Altmark gas field in Germany (classified as subarkoses to sublitharenites: 39–65 % quartz; 1–14 % lithoclasts; 2–17 % K-feldspar; 4-5% calcite.), Pudlo et al. (2012) concluded that the near wellbore area, ongoing scCO2 supply may force intense carbonate dissolution, but at some distance calcite will precipitate in the reservoir. Such spatial differences of potential processes are also relevant for the migration of detached (clay) fibres and thus in pore throat plugging, further impairing reservoir permeability. Ganzer et al. (2014) made similar conclusions by subjecting specimens of the Rotliegend sandstone (Altmark gas field, Germany) to flood of liquid CO2.

The review carried out by Rohmler et al. (2016) indicated that the greatest response to CO2 treatment is expected for carbonate reservoirs (and for carbonate-cemented sandstones, though to a lesser extent) flushed by a CO2-saturated (acid) brine under high injection rates. Under these conditions: i) high-porosity / permeability dissolution channels can be formed, primarily in the vicinity of the injection well; ii) the formation of such dissolution channels may in turn enhance flow, which may lead to further reaction, and so on; iii) it is to be expected that such structures might eventually

collapse under the confining pressure, which could lead to the acceleration of reservoir compaction, and decreased flow rates.

This conclusion indicates a general behavior, based on a large number of experiments. Next step is the correlation of this outcome with the change in mechanical properties of the rock.

Kim & Makhnenko (2022) reviewed some experiments and observed that generally, there is an agreement that CO2 treatment induces a considerable chemical reaction that decreases the stiffness of limestones by 20–30% due to dissolution (Alam et al. 2014; Bemer and Lombard 2010; Grombacher et al. 2012; Kim et al. 2018; Vanorio et al. 2011; Vialle and Vanorio 2011), while on the other hand, some cases reported no chemical effect (Liteanu et al. 2013). At the same time, the chemical effect of CO2 treatment on the compressibility is shown to be weak for silica-cemented sandstones (Lei and Xue 2009; Vanorio et al. 2011), while the ambiguous results were reported for carbonate cemented silica-rich rock (Aman et al. 2018).

On the other hand, Tarokh et al. (2020) observed that CO2 can interact with brine-saturated host rock and cause microstructural changes that lead to alterations in poromechanical properties of the rock. The effect is well pronounced in carbonate-rich rock, but observations on silica-rich reservoirs are ambiguous.

In the following the results of some experiments are analyzed in detail, in order to outline some ambiguous results and their causes.

Rimmelé et al. (2010) noticed that exposing the Lavoux limestone (99% calcite) samples and the Adamswiller sandstone (quartz 71%, feldspar 9% with little alteration, clay 11%, mica 5%, and traces of apatite, iron and titanium oxides) samples to scCO2 or CO2-rich water under no-flow conditions for one month, did not cause relevant variation in the uniaxial compressive strength and deformation modulus.

Mikhaltsevitch et al. (2014) found that scCO2 injection does not affect the elastic properties of water-saturated Donnybrook sandstone (Quartz 60 %, Siderite 1.7 % Microcline 5.4 %, Plagioclase 9.4 %, Kaolinite 22.8 %), obtained at seismic and ultrasonic frequencies.

Ojala (2011) performed Brazilian tests on samples of Castlegate sandstone (70% quartz, 30% feldspar and small amounts of clay), Bentheimer sandstone (95% quartz, 2% altered feldspars and 3% clay) Pierre shale (41% clay, 32% quartz & feldspar and 15 % calcite) and carbonate rocks (Austin chalk and Lixhe chalk). The author concluded that the tensile strength of the sandstone, shale and chalk is not markedly affected by the presence of CO2.

Hangx et al. (2013) carried out triaxial creep experiments (brine and CO2-rich brine) on samples of poorly consolidated, carbonate- and quartz-cemented Captain sandstone. The composition of the rock is quartz(78.1 wt%), feldspar (5.7 wt% K-feldspar; 5.6 wt% plagioclase), and clays (7.6 wt%; mainly kaolinite), with ~0.3% calcite. The purpose of the study was to investigate the effect of carbonate cement dissolution on mechanical and ultrasonic properties, as well as on the failure strength of the material. They indicated that the small amount of carbonate present in the starting material was completely dissolved after several weeks of flow-through with CO2-saturated brine. They noticed formation of holes in the post-experiment samples, suggesting dissolution of calcite. Though calcite dissolution was observed, grain-to-grain contacts appeared to be sufficiently quartz-cemented to prevent significant weakening of the material. The authors observed that after flow-through with brine and CO2-saturated brine, the mechanical parameters did not differ significantly from those prior to flow. The authors concluded that the continuous flushing of the material with CO2-saturated brine, and the concomitant removal of calcite, does not affect material strength or elastic properties.

We noted that the conclusion reported by Hangx et al. (2013) and related to the rock strength is just based on two tests on CO2 exposed samples (Figure 5). The results of these two tests are in agreement with the strength of unexposed samples. However, more strength data of CO2 exposed sample should be used to definitely conclude that the strength of the Captain sandstone is not affected by CO2 flushing. In fact, data scattering is very common in tests carried out on CO2 exposed samples.

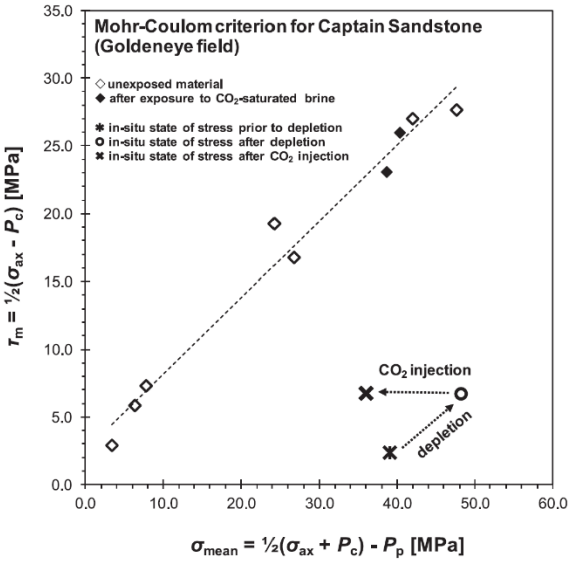

Figure 5. Strength of Captain sandstone for unexposed and CO2 exposed samples (Hangx et al., 2013).

Grgic 2011, conducted triaxial tests on Lavoux limestone in both isotropic and deviatoric loading conditions at temperatures of T= 30–70 °C and for CO2 pressures of 4.5–10 MPa and for time durations up to 70 days. They concluded that under closed-flow conditions, the creep deformation is negligible due to a chemical equilibrium and an increase in pH, which inhibits calcite dissolution. However, under dynamic conditions, they observed an increase in creep strain.

Marbler et al. (2013) carried out triaxial tests on three sandstones: Bunter silicatic (quartz 75%, microcline 20%, clay minerals 3-4%: kaolinite, illite, smectite), Bunter carbonate (quartz 60%; calcite 25%; orthoclase, plagioclase; clay: 3-4 % illite, smectite, kaolinite; muscovite 1%; siderite) and Upper Rotliegend carbonate-silicate (quartz 70%; orthoclase; calcite 4-5%; muscovite 1-2 %; clay minerals 3%: kaolinite, illite, smectite; barite).

The samples were prepared to represent different saturation levels (air dry, partly H2O-saturated and brine-saturated by vacuum) in order to systematically investigate the in situ expected reaction zones with different conditions of brine/gas saturation within the reservoir formation during the CO2 injection. The samples were exposed to brine and scCO2 for 2-4 weeks.

The results of triaxial tests of untreated and CO2 exposed specimens of Bunter sandstones are shown in Figure 6. The figure clearly indicates that at high effective confining pressure (about 10 MPa) there is a drop in strength in the dry specimens, more pronounced in the carbonate sandstone.

The drop in strength at high confinements also occurs when the specimens are fully brine saturated. Finally, the strength of CO2 treated specimens is definitely lower in two cases for the silicate sandstone. Just one test of the CO2 treated carbonate sandstone is reported. The result of this test indicates a reduction in strength. In overall, the results of these tests show a quite high data scattering. This scattering, in particular for the reduction in strength at high confinement, can be attributed to rock damage before testing induced by the process of coring and specimen preparation and/or lithological varieties of the sandstone texture, pore space distribution and mineralogical composition within the samples.

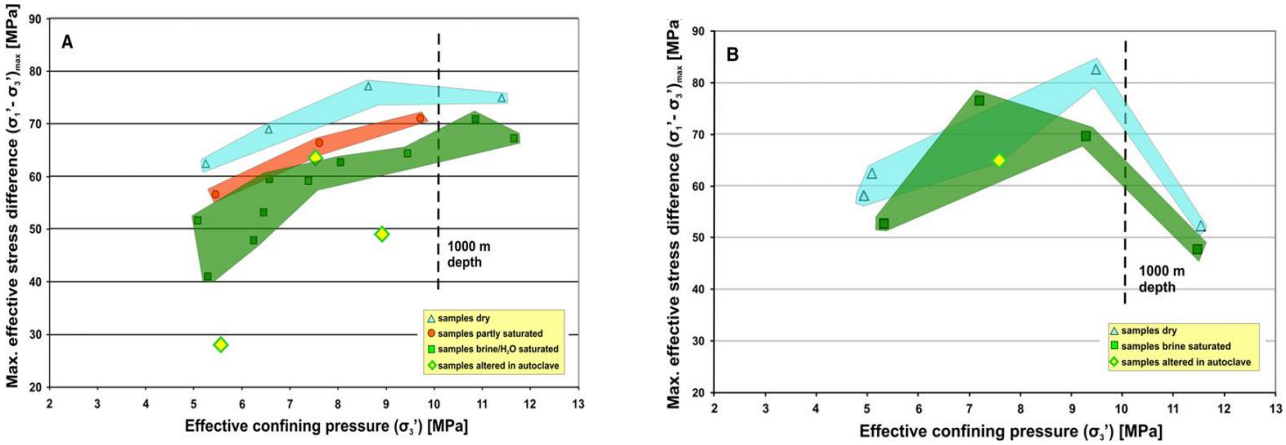

Figure 6. Results of triaxial tests of untreated and CO2 altered specimens of Bunter sandstones. Left: silicate Bunter; Right: carbonate Bunter (Marbler et al., 2013).

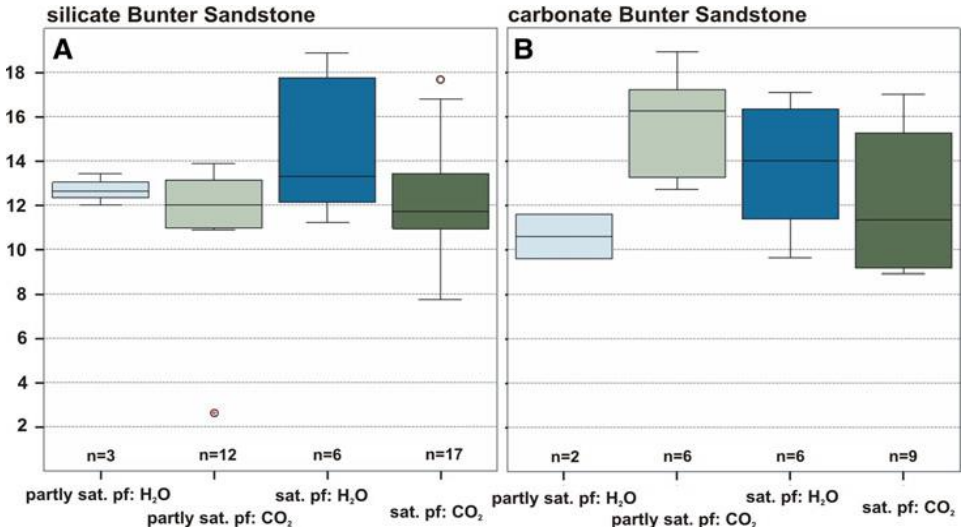

Figure 7. Deformation moduli of untreated and CO2 altered specimens of Bunter sandstones. Left: silicate Bunter; Right: carbonate Bunter (Marbler et al., 2013).

The elastic behavior of the carbonate sandstone samples and silicate sandstone samples is shown in Figure 7. Figure 8 shows the summary of the elastic and strength properties determined with the triaxial tests. To our knowledge it is not clear the technique of measurement used for the determination of the elastic moduli.

Table 2 Shear parameters friction angle (φ'), cohesion (c') and the uniaxial compressive strength (σ_u) as well as deformation properties (modulus of deformation) of differently treated samples from silicate and carbonate "Bunter sandstone" samples

Lithology	Saturation level, pore pressure fluid	Eff. int. friction angle φ' (°)	Eff. cohesion c' (MPa)	Uniax. compress. strength (MPa)	Modulus of def. (GPa)
Silicate "Bunter" sandstones	H_2O sat., pf: H_2O	40.1	8.4	36.1	10.8
	Part. sat., pf: H_2O	44.4	6.1	29	12.7
	Brine sat.; pf: CO_2	33.3	10.9	40	12.7
	Part. sat.; pf: CO_2	33.8	13.6	50.9	13.1
	Altered; pf: CO_2	58.8	0	0	10.3
Carbonate "Bunter" sandstones	H_2O sat., pf: H_2O	42.5	7.5	34.1	13.7
	H_2O sat.; pf: CO_2	49.9	2.9	15.9	12.6
	Part. sat.; pf: CO_2	45.9	6.7	33.1	15.5
	Brine sat.; pf: CO_2	52.3	1.9	11.1	11.9
	Altered; pf: CO_2	n.d.	n.d.	n.d.	11.1
Silicate and carbonate "Rotliegend" sandstones	H_2O sat., pf: H_2O	56.8	9.2	61.7	16.7
	Brine sat.; pf: CO_2	nd	nd	nd	22.4
	Altered; pf: CO_2	nd	nd	nd	14.7

nd not determined due to insufficient amount of data

Figure 8. Properties determined with the triaxial tests for unaltered and CO2 altered samples (Marbler et al., 2013).

The analysis of Figures 7 and 8 indicates that the lower deformation moduli are obtained in pure CO2 altered samples for all sandstones. A comparison between H2O saturated and pure CO2 altered samples indicates a -5% decrease in silicate Bunter sandstone, -19% decrease in carbonate Bunter sandstone and -12% decrease in silicate/carbonate Rotliegend sandstone. On the other hand, a comparison between H2O saturated and brine saturated-CO2 samples indicates a 18% increase in silicate Bunter sandstone, -13% decrease in carbonate Bunter sandstone and 34% increase in silicate/carbonate Rotliegend sandstone. In conclusion, the reduction of the deformation moduli, with brine saturated-CO2 samples, occurs only in the carbonate Bunter sandstone, while the other two sandstones exhibit a relevant increase in the deformation moduli.

The analysis of the strength properties indicates that the cohesion and the friction angles were not determined in pure CO2 altered samples. This fact can be maybe attributed to the data scattering reported in Figure 6, which makes difficult the regression for data fitting.

A comparison of the strength variation between H2O saturated and brine saturated-CO2 samples indicates an increase (+30%) in cohesion and a decrease in friction angle (-17%) for the silicate Bunter sandstone; and a decrease in cohesion (-75%) and an increase in friction angle (23%) for the carbonate Bunter sandstone.

The results of these tests carried out by Marbler et al. (2013) are scattered and a clear rock behavior is sometimes difficult to be identified. In overall, these results indicate that pure scCO2 reduces the deformation moduli independently of the composition of sandstones. The effect of brine saturation-CO2 decreases the deformation modulus in carbonate sandstone and increases the moduli for the other two sandstones. The strength properties, cohesion and friction, have a mixed variation in the carbonate and silicate sandstones.

Espinoza et al. (2018) investigated the changes in geomechanical properties caused by CO2-charged brine over geologic time from rocks in a sedimentary system at the Crystal Geyser field- Utah, which has been widely utilized as a CO2 sequestration analog. They performed triaxial experiments on Entrada sandstone (~55 wt% Quartz, 24 wt% clays, 14 wt% carbonates, 7 wt% K-feldspar, plus trace minerals), Summerville siltstone (matrix composed by very fine grained quartz grains in a matrix formed principally by sparry calcite, illite-smectite, and feldspar; carbonate content from 23 wt% to 43 wt%), and Mancos shale (matrix dominated by fine quartz 64 wt%, feldspar and clay minerals: illite, illite/smectite, chlorite/smectite, and kaolinite) specimens reacted with CO2-brine mixture. The results showed that the strength and stiffness of sandstone and siltstone decreased due to mineral dissolution, while the stiffness of Mancos shale increased due to precipitation of calcite minerals. The authors concluded that the dissolution and precipitation of minerals due to CO2-acidified brine injection could decrease or increase the strength and stiffness of the rock, depending on the particular material and its composing minerals. Furthermore, Espinoza et al. (2018) observed that predominantly quartzitic sandstones and unconsolidated sands are expected to have minor chemo-mechanical alteration when exposed to CO2 due to a lack of reactive minerals. Sandstones with "CO2-weak" intergranular cements appear to be the most easily alterable type of rock with respect to geomechanical properties, as even minor alterations can have a large impact on geomechanical properties dependent on cementation.

Rathnaweera et al. (2015) carried out uniaxial compressive tests on Hawkesbury sandstone (85% quartz, 5% calcite, 1% siderite, 1% mica, 5% kaolinite, 2% anatase and 1% amphibole) and reported the dissolution of calcite and corrosion of quartz mineral, which resulted in a mechanical weakening.

The results of uniaxial compressive tests are shown in Figure 9. The figure indicates that the reduction in the uniaxial compressive strength due to CO2 exposure decreases with the NaCl content with a maximum for fresh water. The Young modulus of the CO2 exposed rock is constant from fresh water to the maximum NaCl content, but Young modulus of the non-CO2 treated rock increases. The Poisson ratio is always reduced after CO2 treatment but shows an increase from fresh water to the maximum NaCl content, as for the unexposed rock.

The degree of salinity of the pore fluid also greatly influences the CO2 adsorption-induced strength reduction in Hawkesbury sandstone. For example, super-critical CO2 saturation causes around 32.89%, 17.65%, and 14.75% uniaxial compressive strength reductions and 1.8%, 57.45%, and 92.3% Young's modulus reductions in brine-saturated Hawkesbury sandstone with 10%, 20%, and 30% NaCl concentration brines, respectively.

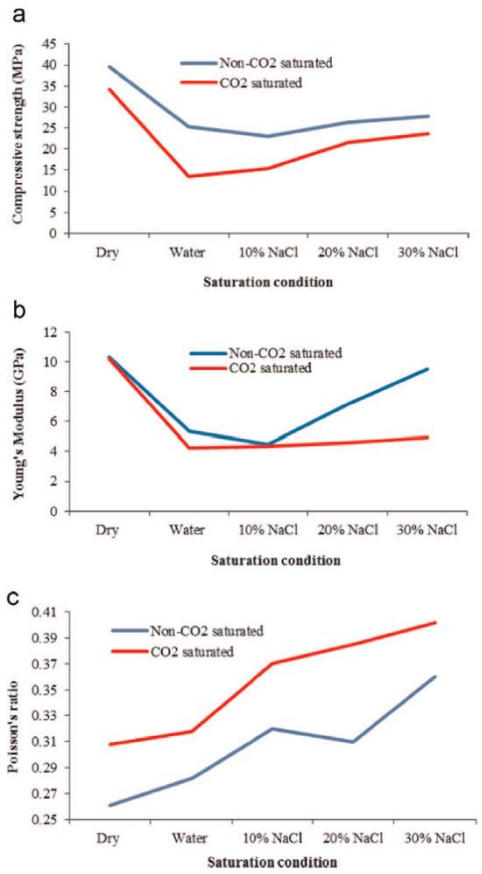

Figure 9. Effects of CO2 injection on Hawkesbury sandstone (a) average unconfined compressive strength, (b) Young's modulus and (c) Poisson's ratio. (Rathnaweera et al., 2015).

Rathnaweera et al. (2015) detected stress thresholds for crack initiation and progression in water and brine-saturated Hawkesbury sandstone exposed to scCO2 injection. Their AE results indicated the weakening effect of CO2 injection, resulting in considerable influence on crack initiation and propagation in the rock.

The analysis of three studies (Fuchs et al., 2019; Shi et al., 2019; Harbert et al., 2020) carried on Mt Simon sandstone are analyzed and compared in the following.

Fuchs et al. (2019) evaluated the effects of geochemical reactions on geomechanical integrity of siliciclastic reservoir samples obtained from the Mt. Simon formation. Rock samples were aged 4 or 8 weeks in CO2-saturated brine under reservoir conditions, and in N2-saturated brine as a control. The retrieval depth of the samples was 2111.35 m. The mineralogical analysis carried out at the 2118.4 m interval includes quartz (79%), potassium feldspar (K-feldspar, 15%), sericite (1%), illite-smectite (4%), iron oxide-illite (1%), and other trace minerals (Freiburg et al., 2014). In the formation, quartz and feldspar contents were reported ranging from 40 to 80% and 13–22%, respectively, with clays content reaching as high as 28% for different samples between depths of 2082.7 to 2131.5 m. Figure 10 shows the mineralogical data of initial, N2-aged and Co2-aged samples. Post-aging revealed more extensive micro-fracture development along horizontal bedding planes at grain edges in CO2 versus N2-aged samples. CO2-aged samples showed porosity increase from 8.1% to 15.8%. They observed the loss of clay cementation, greater exposure of quartz and K-feldspar grains, and apparent surface roughening in CO2-aged samples, but not in N2- aged samples. Finally, the strength of the sandstone pre and post exposure to N2 and CO2 was evaluated with the scratch test. They noticed that fracture toughness was reduced by 32.1% after 4 weeks in scCO2-saturated brine and 69.5% after 8 weeks (Figure 11). The primary reason for weakening appears to be detachment of clays from quartz and feldspar grain surfaces, resulting in weakening of the rock matrix.

Table 2
XRD Mineralogical Data for initial, 8-week CO_2-aged sample (MS1) and 8-week N_2-aged sample (MS4). Tr indicates < 0.5.

Mineral	Formula	MS1 Initial % composition	MS4 (N_2) Aged % composition	MS1 (CO_2) Aged % composition
Quartz	SiO_2	75.7	66.1	60.6
K-Feldspar	$KAlSi_3O_8$	17.0	20.4	25.0
Calcite	$CaCO_3$	0.8	1.2	1.1
Dolomite, Fe	$CaFe(CO_3)_2$	Tr	0.5	0.6
Illite	$(K,H_3O)(Al,Mg,Fe)_2$ $(Si,Al)_4O_{10}[(OH)_2{\cdot}n(H_2O)]$	2.8	5.0	5.4
Illite/ smectite	$(Na,Ca)_{0.33}(Al,Mg)_2(Si_4O_{10})$ $[(OH)_2{\cdot}nH_2O]$	3.1	5.8	4.4
Hematite	Fe_2O_3	0.6	1.0	0.8
Halite	NaCl	Tr	Tr	2.1

Figure 10. Mineralogical data of initial, N2-aged and Co2-aged samples (Fuchs et al., 2019).

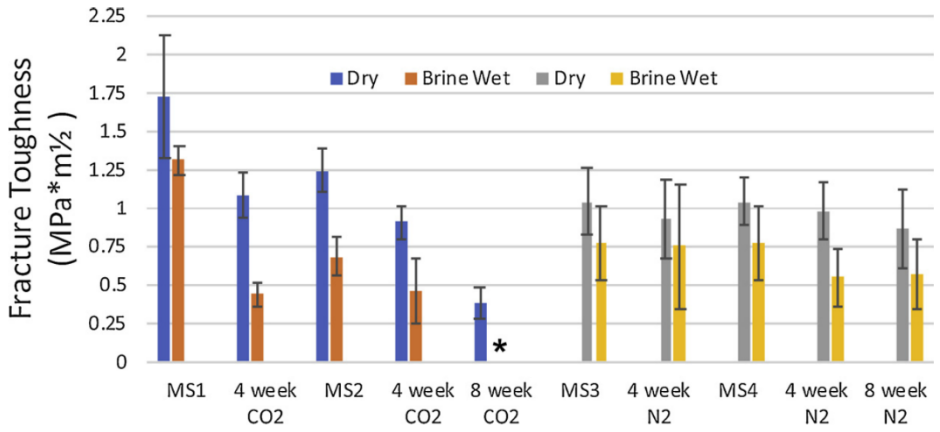

Figure 11. Fracture Toughness of Mt Simon sandstone pre-post exposure to N2 and Co2 (Fuchs et al., 2019).

Shi et al. (2019) carried out laboratory tests on Mt Simon sandstone samples from 2110.4–2111.4 m depth (the same sandstone investigated by Fuchs et al., 2019). They reported the mineral composition from a depth of 2120 m: Quartz 80%, K-feldspar 8%, Plagioclase 4%, Ankerite/Fe-dolomite 1%, Dolomite 1%, Pyrite 1%, Barite 1% and Clay 7% (Illite-smectite 52% Illite 47%, Chlorite 1%).

The authors noticed that all porosities increase after exposure, perhaps suggesting that for these rock samples and the relatively short period of exposure (1-2 weeks) to brine/CO2 mixtures, mineral dissolution dominates over secondary precipitation, resulting in an increase in porosities. Figure 12 shows the variation of the porosity in the samples in pre and post CO2 exposure. The relative change varies from 1.1 % to 14.9 %.

Table 3
Porosity of the core samples.

Sample	Porosity Fresh (%)	Porosity Aged (%)	Aging (weeks)	Relative Change (%)
6927-A1	20.9	21.5	1	2.9
6927-A2	23.8	25.8	2	8.4
6927-A3	25.3	–	–	–
6925-A1	26.3	26.6	1	1.1
6925-A2	19.2	20.5	2	6.8
6924-A1	20.7	21.6	1	4.3
6924-A2	21.5	23.2	2	7.9
6927-B1	16.0/15.8[a]	–	–	–
6927-B2	14.7	–	–	–
6927-B3	15.0	15.3	1	2
6927-B4	14.8	17.0	2	14.9
6927-C1	23.6	24.2	1	2.5

[a] Repeated measurement (after 2 month) to validate repeatability of the porosity measurements.

Figure 12. Porosity of the Mt Simon sandstone in pre and post CO2 exposure (Shi et al., 2019).

Because of the opening of the pore throats due to mineral/clay dissolution, the permeability of the cores also increases after exposure. The porosity of the 6927-B4 core increased by ~14.9% upon exposure to CO2/brine. The (liquid) permeability of the same core increased by ~ 255%. Furthermore, after the dynamic testing of the mechanical properties for each of the two cores (6927-B2 and 6927-B4) was completed, the permeability for each core was measured at various confining pressures. Figure 13 shows these changes in permeability. The figure indicates that the differences in the permeability values measured before and after the mechanical property testing are due to irreversible changes. The irreversible changes are probably due to pore collapse which results in compaction/re-packing of the grains as a result of the high applied effective stresses.

Table 4
Permeability measurements before and after exposure to CO_2/brine.

Sample	Fresh sample (mD)	Aged sample (mD)	After mechanical testing (mD)
6927-B1	9.0[a]	–	–
6927-B2	9.8[a]	–	5.0[b]/6.8[c]
6927-B4	10.6[a]	37.7[a]	6.6[b]/8.4[c]

[a] Measured with a confining pressure of 1.38 MPa (USC set-up).
[b] Measured with a confining pressure of 2.76 MPa (USC set-up) after mechanical testing.
[c] Measured with a confining pressure of 1.38 MPa (USC set-up) after mechanical testing.

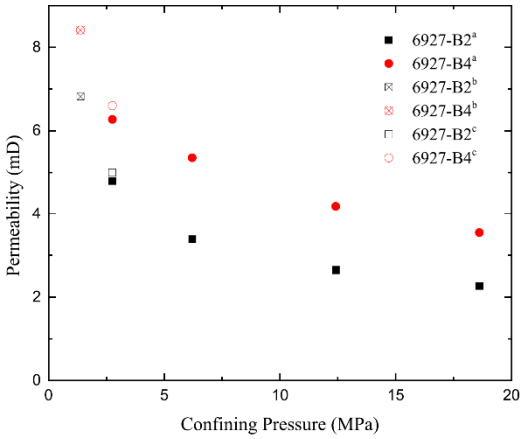

Figure 13. Changes in permeability in pre and post CO2 exposure and after mechanical tests. The graph (right side of the figure) shows the permeabilities of the 6927-B2 (fresh) and 6927-B4 (aged) cores after the mechanical tests. a Measured with confining pressure from 2.76 MPa to 18.62 MPa (NETL set-up); b Measured with confining pressure of 1.38 MPa (USC set-up); c Measured with confining pressure of 2.76 MPa (USC set-up). (Shi et al., 2019).

These high-applied effective stresses probably affected the results of the measured ultrasonic velocities (compression-wave velocities and shear-wave velocities) for the estimation of dynamic Young modulus and bulk modulus. Figure 14 shows the Young modulus vs effective confinement pressure for fresh and aged conditions. The figure shows the occurrence of hysteresis during the loading/unloading cycles. Furthermore, at the end of the first loading/unloading cycle, the dynamic Young modulus does not return to its original value. This is more obvious for the aged sample 6927-B4 signifying, potentially, that plastic (irreversible) deformation of the core pore structure has occurred, as commented above.

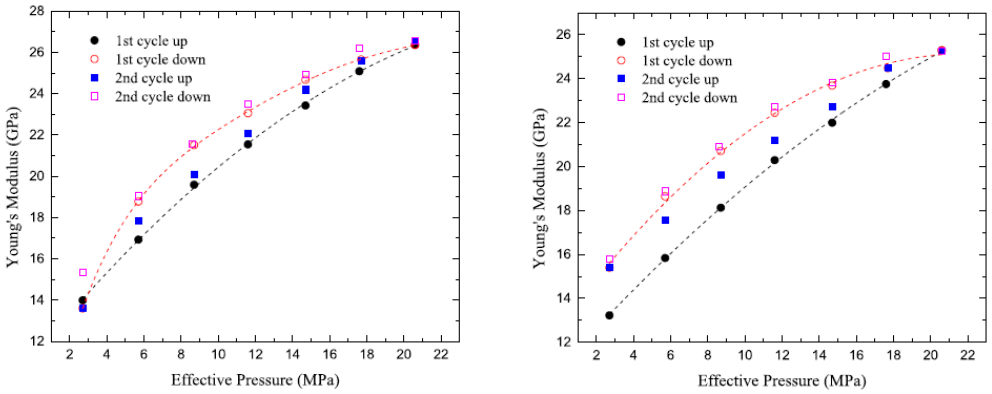

Figure 14. Young Modulus vs effective confinement pressure for fresh 6927-B2 (left) and aged 6927-B4 (right) measured during 2 loading/unloading cycles at different effective confinement pressure. (Shi et al., 2019).

The Authors calculated the average dynamic Young modulus during the first cycle for core 6927-B2 and its equivalent incubated counterpart (core 6927-B4). The dynamic Young modulus of the aged sample is clearly lower than that of its fresh counterpart for the whole range of the applied effective stress. The authors reported that the relative difference is −5.8%, by averaging the Young moduli of all the effective confinement pressures. A similar behavior is exhibited by the bulk modulus, by averaging the bulk moduli of all the effective confinement pressures, the relative difference is -6.7 %. The results obtained by Shi et al. (2019) may lead to some uncertainties related to the change in elastic properties from fresh to CO2 exposed Mt Simon sandstone. The changes seem to be mainly induced by elasto-plastic deformation of the rock pore structure. However, the irreversible deformation seems to affect also the fresh rock. We can conclude that these properties are no longer elastic.

Harbert et al. (2020) carried out a study to quantify geochemical reactions of CO2 and brine with subsurface samples taken from the Mt. Simon sandstone (the same sandstone investigated by Fuchs et al., 2019 and by Shi et al. 2019) and identify any potential alterations of the geomechanical rock properties that could lead to changes observable in seismic monitoring or result in changes of micro seismicity. Two Mt. Simon sandstone samples from 2109.0 m and 2111.1 m depth were exposed to scCO2 dissolved in brine at in situ reservoir conditions for one month.

The mineral composition of the rock was determined in VW1-6919 sample: quartz (76 %), K-feldspar (17 %), and illite-smectite clays (4%). This composition differs from that of Shi et al. (2019) mainly in K-feldspar content.

They measured ultrasonic velocities (compression-wave velocities and shear-wave velocities) for the estimation of dynamic Young modulus, bulk modulus, shear modulus, λparameter, and Poisson ratio. They also estimated the brittleness of the rock pre and post scCO2 exposure.

The tests were carried out in the range of effective confinement pressure 4.4 MPa -21.4 MPa. The highest value is about equal to that used by Shi et al. (2019) that induced irreversible deformation.

Harbert et al. observed different behavior in the two samples. In sample VW1-6926 it appears that geochemical alterations promoted by CO2/brine and mineral framework interactions reduced mineral strength along grain boundaries and promoted fracture propagation or created a new fracture along a bedding plane, which increased permeability by 205 %. They measured an 8% increase in porosity. This increase in permeability seems to be mainly related to the generation of a new fracture. On the other hand, the 255% increase in permeability obtained by Shi et al. (2019) on sample 6927-B4 was related to the increase of porosity. In sample VW1-6926 a -12 % decrease in brittleness, a -29% decrease in Young modulus, and a 15% increase in Poisson ratio were observed. In contrast, sample VW1-6919, showed -8% decrease in brittleness, -9% decrease in porosity, 0% change in permeability, 19% increase in Young modulus, 33% increase in Poisson ratio after CO2/brine exposure. This sample exhibits a different variation of the properties compared to the sample VW1-6926, especially in porosity. Figure 15 shows the variation of the Young modulus, Poisson ratio and Lamé constants of the two samples in pre and post exposure conditions.

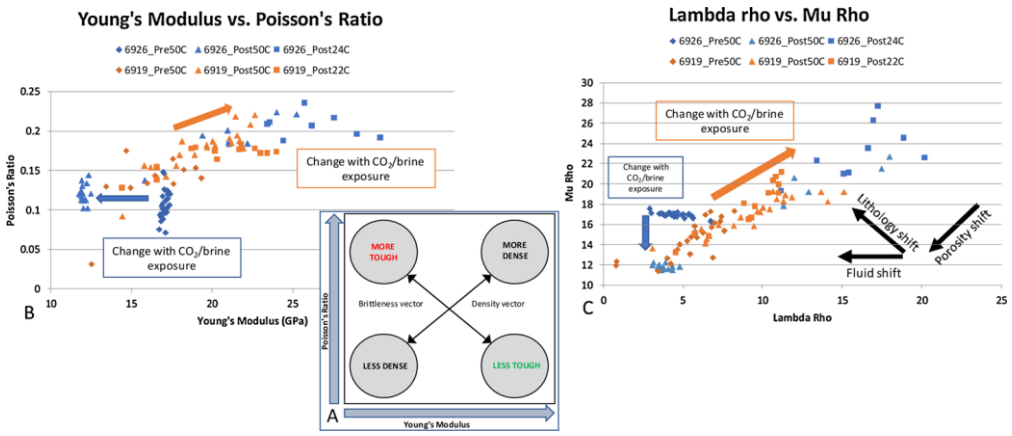

Figure 15. Elastic properties of the two samples of Mt Simon sandstone before and after CO2 exposure (Harbert et al., 2020)

The two samples, from the same formation, displayed different changes, emphasizing the importance of understanding geochemical processes and formation heterogeneity. Harbert et al. concluded that framework composition, porosity, heterogeneities, effective pressure, and reactive geochemistry are first order controls on trends in the elastic properties.

The results of the study carried out by Harbert et al. (2020) may lead to uncertainties related to the obtained data, mainly for the higher effective confinement pressures, as for the results of Shi et al. (2019).

The three studies on Mt Simon sandstone (Fuchs et al., 2019; Shi et al., 2019 and Harbert et al., 2020) indicate that more experimental data are needed. These data should be obtained through more controlled conditions in order to avoid the superimposition of mechanical effects that are unwanted.

Finally, it is worth to mention that the CO2 injection zone of the Illinois Basin Decatur site was 2128–2148 m. The Mt Simon sandstone cores were retrieved in the three previous studies (Fuchs et al., 2019; Shi et al., 2019 and Harbert et al., 2020) at a maximum average depth of 2111 m. Fuchs et al. (2019) indicated that it is highly unlikely that CO2 contacted the core material during injection.

Tarokh et al. (2020) carried out a broad range of experiments on Berea sandstone (minerals vary between 79 and 90 wt% for quartz, 4 and 7.2 wt% for mica/illite, 3 and 6.6 wt% for kaolinite, 1.8 and 3.5% for K-feldspar, and 0.8 and 2.5 wt% for albite).

The tests were carried out on specimens water-saturated in three different states: pristine, thermally damaged, and liquid CO2 treated-thermally damaged. Tarokh et al. (2020) carried out drained and

undrained poromechanical tests, ultrasonic velocity measurements, acoustic emission (AE), X-ray diffraction (XRD), and petrographic analyses.

They observed that there are minor differences between pristine, heat damaged, and CO2 treated damaged samples in terms of carbonate and clay presence that can be attributed to clay mineral stability due to different treatment.

The authors noticed that combined thermal damage and CO2 treatments increased the permeability (up to 100%) and porosity (by 10%) but did not significantly affect the static and dynamic elastic constants (not more than 15%) nor inelastic fracture processes (based on acoustic emission count). The uniaxial strengths of 29.6 and 29.9 MPa (pristine) and 31.3 and 32.6 MPa (damaged) were obtained, suggesting insignificant effects of the heat treatment on the uniaxial strength of Berea sandstone. The authors noticed that the results for strength of CO2 treated damaged specimens are less consistent (22.0 and 30.7 MPa) and do not allow to make an unambiguous conclusion on the effect of CO2 injection. While the CO2 treatment could definitely cause more defects to appear in rock, it has to be noted that failure during a uniaxial compression test is sensitive to small defects within the samples and to sample selection and preparation.

On the other hand, the poroviscoelastic behavior of the Berea sandstone is noticeably affected by CO2 treatment. The time-dependent deformation of water saturated specimens under constant load was more than twice faster compared to pristine and damaged states.

Kim & Makhnenko (2022) explored the chemical effects of liquid CO2 treatment on the poroviscoelastic and hydraulic properties of three rocks. Berea sandstone (85–90% quartz with kaolinite, K-feldspar, and muscovite traces), Apulian limestone (95-98 % soft calcite), and Indiana limestone (97% calcite with minor quartz, aluminum oxide, and sulfur portions) are selected as representative reservoir materials. CO2 treatment increases the bulk modulus of the sandstone and limestones by 15–20%. The undrained response is characterized through measurements of Skempton's B coefficient, which decreases for Berea sandstone, but increases for the limestones, indicating the effect of dissolution and precipitation induced by CO2. For calcite-rich rock, the porosity and solid bulk modulus increase by 4–6% and 20%, respectively, while these parameters remain unchanged for silica-rich rock. As the time-dependent behavior is measured indirectly by monitoring the pore pressure buildup under an undrained condition, the CO2 treatment appears to significantly facilitate the viscous response by 50–60% for all materials.

The conditions of the tests on Berea sandstone carried ou by Tarokh et al (2020) and Kim & Makhnenko (2022) with liquid CO2 are well describe in both studies, allowing a quite good comparison between the obtained results. The results of these studies are in agreement.

Hu et al. (2016) investigated the mechanical behavior of a sandstone (from Zigong, Sichuan Province, China) in the conditions of mono-phase fluids and bi-phase fluid. The composition of the sandstone is: 50.73% quartz, 34.01% albite, 10.59% calcite, 3.32% illite, and 1.36% montmorillonite.

The mono-phase true triaxial tests were conducted for dry sandstone or sandstone containing N2, scCO2, or H2O to determine their strength and stress-strain characteristics under different pore fluid conditions and to reveal the mechanisms underlying the actions of different pore fluids on rock mechanical behaviors. The bi-phase true triaxial tests were conducted for samples with scCO2-H2O biphase pore fluid

The results of the true triaxial tests are shown in Figure 16. The figure indicates that the case of dry rock exhibits the highest strength, as expected. Furthermore, the strength of rock was affected by the high-pressure of gas and water and their effective extent ranked in descending order as H2O > CO2 > N2. The behavior exhibited during the tests is brittle.

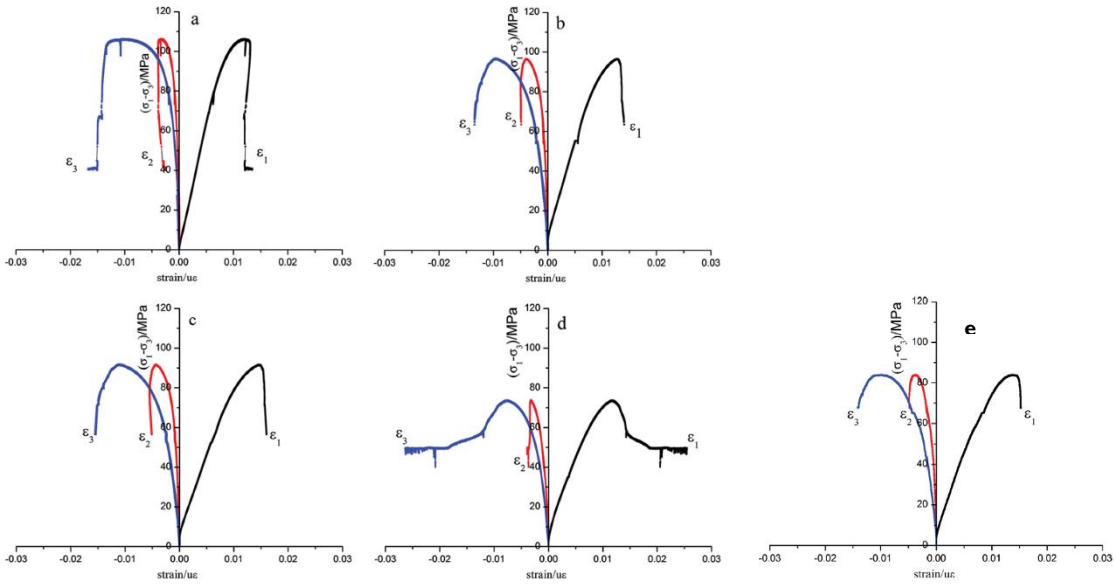

Figure 16. Results of the triaxial compression experiments on Zigong sandstone subject to monophase pore fluid. (a) dry ; (b) N2-bearing sandstone; (c) CO2-bearing sandstone; (d) H2O-bearing sandstone; (e) CO2-H2O biphase fluid. (Hu et al., 2016).

In particular, the peak stress was 105.235 MPa for dry sandstone and 96.565 MPa, 91.588 MPa and 73.774 MPa for sandstones containing N2, CO2 and H2O, respectively. This result indicates that the nitrogen N2 lightly interacts with the rock minerals and the reduced strength with respect to dry conditions is due to pore pressure. Furthermore, the pure CO2 affects lightly the rock strength, compared to H2O.

The calculated elastic modulus at the linear elastic stage was 11.681 GPa, 10.901 GPa, 9.928 GPa and 8.883 GPa for dry sandstones and for sandstones containing N2, CO2 and H2O, respectively.

Finally, the bi-phase fluid conditions with CO2 pressure at 10 MPa and H2O pressure at 8.5 MPa, shows that the measured peak stress of sandstone was 84.388 MPa, greater than that of 73.774 MPa for H2O-bearing sandstone, but smaller than that of 91.588 MPa for CO2-bearing sandstone.

In addition, the elastic modulus of the bi-phase fluid coupled sandstone at the linear elastic stage was 9.064 GPa, slightly greater than that of water-bearing sandstone, but significantly less than that of the supercritical CO2 bearing sandstone, indicating that the impact of H2O on the elastic modulus of the sandstone was significantly greater than that of supercritical CO2.

The effect of CO2 impurities on the mechanical properties of sandstones was studied by Erickson et al. (2015). They carried out triaxial tests on specimens of Bunter silicatic sandstone, Bunter carbonate sandstone and Upper Rotliegend carbonate-silicate sandstone (Germany). The mineralogical composition of these rocks is reported above, in the study of Marbler et al. (2013). Some samples were saturated with brine (2 mol/l NaCl solution). Some samples used for triaxial tests were first exposed to scCO2 (+impurities) and brine during experiments for 1 month in an autoclave system. Consequently, the authors investigated the behavior and the reactions of unaltered rocks in dry and in saline-saturated states and of artificially altered rocks (scCO2) in the saline-saturated state.

Figure 17 shows the results of the triaxial tests in terms of deformation moduli in unaltered and altered conditions for the three sandstones. The moduli are normalized to the modulus at treatment with pure scCO2 (=100 %). Because the increased stress level induces plastic deformation and reduces elastic behavior, the deformation modulus at the initial loading decreases in case of elevated stress levels, i.e., comparing mean values of the deformation modulus at 0.3 and 0.6 of the maximum deviatoric stress and at 0.7 and 0.9 of the maximum deviatoric stress, respectively.

The figure shows that differences due to saturation state are neither uniform nor uniformly modified. One should take into consideration the wide variety of natural deformability of the different rock types. More pronounced are the differences in case of alteration: The small selection of altered samples shows clearly reduced deformation moduli compared to the unaltered samples.

In general, the deformation modulus was most reduced if impure scCO2 had invaded the pores. Independently of original saturation state or preceding alteration, the impure scCO2 generates reduced deformation moduli compared with pure scCO2. The amount of deformation moduli reduction is about -10–40 %.

Erickson et al. noticed that the effective maximum stress differences versus effective confining pressure conditions demonstrated a wide scattering of experimental results.

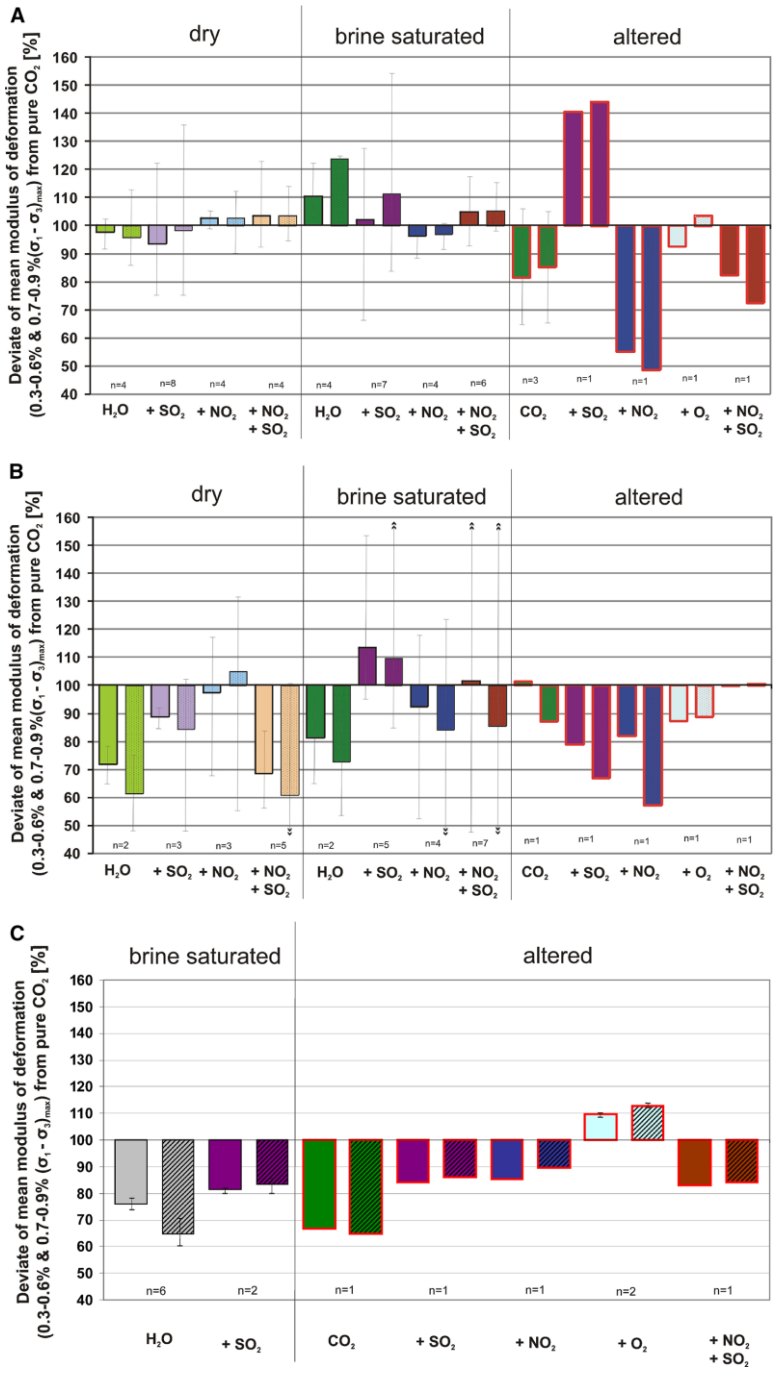

Figure 17. Deformation moduli normalized to the modulus at treatment with pure scCO2 (=100%). The moduli are initial loading determined at different states of saturation and alteration under the influence of scCO2 and defined impurities. Left columns: Deformation modulus between 0.3 and 0.6 of the maximum deviatoric stress. Right columns: (hatched) Deformation modulus. between 0.7 and 0.9 of the maximum deviatoric stress. A) Siliceous sandstone, B) carbonate sandstone and C) siliceous/carbonate sandstone. (Erickson et al, 2015)

Figure 18 reports the strength parameters obtained by data fitting of effective maximum stress differences versus effective confining pressure.

Here we consider as a reference the strength parameters of the case brine fully saturated and H2O pore fluid pressure. For brine-saturated samples, the friction angle consistently reduces with CO2, CO2+SO2 and CO2+NO2 and increases with CO2+SO2+NO2 in the silicate sandstone. . In the carbonate sandstone the friction angle decreases with all impurities except with CO2 (a negligible increase constant). For brine saturated samples the cohesion increases with all impurities and with CO2 (this last result is opposite to that found by Marbler et at. (2013), reported in Figure 5, although the rock is the same) in the carbonate sandstone. In the silicate sandstone, the cohesion increases except for the case CO2+SO2+NO2, where the cohesion reaches the minimum value.

Table 4 Effective strength parameters angle of friction and cohesion of the silicate sandstone (s)

Saturation state	Pore pressure fluid	Angle of friction φ′ (°)	Effective cohesion c′ (MPa)	Uniaxial compressive strength (MPa)
Brine sat.	H_2O	40.1	8.4	36.11
Brine sat.	CO_2	33.3	10.9	40.4
Brine sat.	CO_2 + 500 ppm SO_2	33.2	11.6	42.91
Brine sat.	CO_2 + 100 ppm NO_2	21.2	16.8	49.07
Brine sat.	$CO_2 + NO_2 + SO_2$	44.6	4.1	19.6
Partly sat.	H_2O	44.4	6.1	29.02
Partly sat.	CO_2	33.8	13.6	50.94
Partly sat.	$CO_2 + SO_2$	45.1	5.7	27.59
Partly sat.	$CO_2 + NO_2$	37.7	9.4	38.29
Partly sat.	$CO_2 + NO_2 + SO_2$	44.2	6.5	30.78

Table 5 Effective strength parameters angle of friction and cohesion of the carbonate sandstone (c)

Saturation state	Pore pressure fluid	Angle of friction φ′ (°)	Effective cohesion c′ (MPa)	Uniaxial compressive strength (MPa)
Brine sat.	H_2O	52	1.3	6.57
Brine sat.	CO_2	52.3	1.9	9.66
Brine sat.	CO_2 + 500 ppm SO_2	39.6	7.7	29.99
Brine sat.	CO_2 + 100 ppm NO_2	35.5	5.8	20.91
Brine sat.	$CO_2 + NO_2 + SO_2$	44.2	3	12.8
Partly sat.	H_2O	n.e.	n.e.	n.e.
Partly sat.	CO_2	45.9	6.7	29.62
Partly sat.	$CO_2 + SO_2$	48.6	3.7	17.32
Partly sat.	$CO_2 + NO_2$	55.4	0	0
Partly sat.	$CO_2 + NO_2 + SO_2$	46.3	4.1	18.28

n.e. = not determined

Figure 18. Strength parameters at different states of saturation and alteration under the influence of scCO2 and defined impurities. (Erickson et al., 2015)

As noticed by Erickson et al. (2015), the experimental results in terms of the effective maximum stress differences versus effective confining pressure were affected by a wide scattering. This issue affects the process of data fitting. In conclusion, more tests are required to confirm the variation of the strength parameters at different saturation states and pore pressure fluids.

Other studies have investigated impacts of CO2 injection on the integrity of saline reservoir caprock. Mouzakis et al. (2016) and Miller et al. (2016) studied interaction of CO2 and brine saturated cap rocks. The Gothic Shale and Marine Tuscaloosa experienced silicate and calcite dissolution, and porosity enhancement. The study indicated that porosity increment was not necessarily followed by pore connectivity enhancement, since it was observed that the pore connectivity of Marine Tuscaloosa decreased as the porosity increased. This phenomenon can be attributed to the secondary precipitation of the minerals that clogged pore throats and the expansion of the clay minerals due to CO2 injection (Foroutan et al., 2021).

Hangx et al. (2009 and 2010) investigated the impacts of injecting CO2 on the sealing properties of the Zechstein anhydrite-rich caprock (the Netherlands). The rock contained between 10 and 33 wt% carbonate, most likely dolomite. The samples were dry, pre saturated with CaSO4 solution and exposed to CO2. The authors observed a reduction on the mechanical strength (~ -20% ÷ -10%) of anhydrite on the timescale of the experiments (~5h). They reported that long-term exposure of CO2-caprock could result in 20% porosity enhancement, which can potentially affect the mechanical response and sealing properties of the anhydrite-rich caprock. However, they did not measure the porosity nor the strength in the long term. Hangx et al. (2014) obtained similar experimental results for the strength and observed a small reduction of the deformation modulus (-8%).

Table 1 summarizes the effect of CO2 discussed in the previous paragraphs. The data reported in this table indicate that the effect of CO2 on rock properties is ambiguous, especially for silicate sandstones. These outcomes are quite usual, because rocks are real materials containing heterogeneities at all scales and do not strictly obey to mathematical idealizations. For instance, in the simplest condition of dry rock specimens subject to uniaxial loading, the strength variation can be as high as 30%. The CO2 exposure and brine composition introduces further complex interactions that can amplify the variability of the rock properties. For comparison, the Appendix reports the summary of the review (table) carried out by Rohmer et al. (2016). The analysis

outcomes of these tables indicates that the effects of CO2 injection in real UGS fields must take into account the variability of the mechanical response related to the variability of rock properties. The UGS fields in the Netherlands selected in this KEM for CO2, N2 and H2 injection are located in sandstone and carbonate formations. The UGS in the Norg field (Langelo) is located in the Upper Rotliegend Formation, in both the Lower Ten Boer Member (claystone) of the Silverpit Formation as well as the Slochteren Formation. The UGS in the Alkmaar field is located in the Zechstein carbonate member (Zechstein). The UGSs in the Grijpskerk and Bergermeer fields are located in the Slochteren Formation of the Upper Rotliegend Group.

The Slochteren formation is comprised of fine-to coarse-grained sandstones and locally even conglomerates (Waldmann, 2011). The typical composition of the sandstones is 72%–90% quartz, 8%–25% feldspar (mainly K-feldspar), 3%–10% lithic fragments, and 0.1%–10% clay minerals (kaolinite and illite) (Pijnenburg et al., 2020; Waldmann et al., 2014). The Ten Boer claystone material is composed predominantly of quartz (48 wt%), phyllosilicates (39 wt% in total, with 33 wt% muscovite/phengite and 6 wt% chlorite) and minor feldspar, dolomite, and hematite. The geochemical effects of CO2 injection in the Upper Rotliegend formation is reported above in the papers of Bolourinejad et al. (2014) and Bolourinejad (2015). The authors measured an increase in permeability from 10% to 30%. This outcome should indicate a change in porosity and deformation moduli. The variation of the deformation moduli of this sandstone could be ±30% , according to the results reported in Table 1.

The Carbonate Member of the Zechstein Group is a slightly argillaceous dolomitic limestone or coarse-crystalline dolomite. The geochemical effects of CO2 on the Zechstein caprock are reported above in the studies of Bolourinejad et al. (2014) and Bolourinejad (2015). They noticed and increase in permeability by a factor of 3 to 10 due to the mineral dissolution and they observed that the measured reactive surface areas were significantly higher than what is typically being used in modeling studies, which leads to more dissolution / precipitation of minerals. Furthermore, the results of triaxial tests carried out on CO2 exposed samples of Zechstein caprock (Hangx et al., 2009, 2010 and 2014) indicated a small decrease in the deformation moduli. However, the timescale of the tests was 5hr, which is lower compared to the in site timescale. Given the high carbonate content of the Carbonate Member of the Zechstein Group and according to Table 1, it is probably expected a more significant variation of the deformation moduli with CO2 exposure.

Table 1. Summary of the relative variation of rock properties with CO2 exposure.

FORMATION	Porosity	Deformation moduli	Strength
Mt Simon sandstone (silicate)	**+8% ÷ +16%** (*Fuchs et al., 2019*) **+ 1.1% ÷ +15 %** (*Shi et al., 2019*) **-9% ÷ +8%** (*Harbert et al., 2020*)	**E=-7% and K=-8%** (*Shi et al., 2019*) **E=-29% ÷ +19%** **ν=+15% ÷ + 33%** (*Harbert et al., 2020*)	**FracT=-32% ÷ -69.5%** (*Fuchs et al., 2019*) **BRI=-12% ÷ -8%** (*Harbert et al., 2020*)
Berea sandstone (silicate)	**+10%** (*Tarokh et al., 2020*) **0%** (*Kim & Makhnenko 2022*)	**E=-13% and ν=+18%** (*Tarokh et al., 2020*) **Ks=0% and K=-15%** (*Kim & Makhnenko, 2022*)	**UCS=-18%** (*Tarokh et al., 2020*)
Captain Sandstone (silicate; calcite cement 0.3%)	-	**E< 10% ν<10%** *(Hangx et al., 2013)*	**DEV=0%** *(Hangx et al., 2013)*
Adamswiller Sandstone (silicate)	**+3% ÷ +4%** *(Rimmelé et al. 2010)*	**E=0% ν=0%** *(Rimmelé et al. 2010)*	**UCS=-24% ÷ -8%** *(Rimmelé et al. 2010)*
Bunter sandstone (silicate)	-	**E=-5% ÷ +18%** *(Marbler et al., 2013)*	**c′=+30% and ϕ′=-17%** *(Marbler et al., 2013)*
Bunter sandstone (carbonate)	-	**E=-19%÷-13%** *(Marbler et al., 2013)*	**c′=-75% and ϕ′=+23%** *(Marbler et al., 2013)*
Rotliegend sandstone Germany (silicate-carbonate)	-	**E=-12%÷+34%** *(Marbler et al., 2013)*	-
Hawkesbury sandstone (silicate cemented with minor amount of calcite)	-	**E=-2% ÷--93% ν=+15%** *(Rathnaweera et al. 2015)*	**UCS=-15% ÷ -33%** *(Rathnaweera et al. 2015)*
Indiana limestone (competent rock calcite-rich)	**+6%** (*Kim & Makhnenko, 2022*)	**Ks= -17% and K=-22%** (*Kim & Makhnenko, 2022*)	-
Apulian limestone (soft rock calcite rich 95%-98%)	**+4%** (*Kim & Makhnenko, 2022*)	**Ks=-20% and K=-24%** (*Kim & Makhnenko, 2022*)	-
Lavoux limestone (nearly 100% calcite)	**+2% ÷ +4%** *(Rimmelé et al. 2010)*	**E=0% ν=-30% ÷ +24%** *(Rimmelé et al., 2010)*	**UCS=+13%** *(Rimmelé et al. 2010)*
Summerville siltstone	**+112%**	**E=-86%**	**UCS=-87%**

(quartz grains in a matrix formed by calcite, illite-smectite, and feldspar)	*(Espinoza et al., 2018)*	*(Espinoza et al., 2018)*	*(Espinoza et al., 2018)*
Zechstein anhydrite-rich caprock (the Netherlands)	-	**E=-8%** *(Hangx et al., 2014)*	**DV=-20% ÷ -10%** *(Hangx et al., 2010)* **DV=-8%** *(Hangx et al., 2014)*

Ks= bulk modulus of the solid grains; K=bulk modulus of the porous medium; E=Young modulus or deformation modulus in TXT; ν=Poisson ratio; FracT=fracture toughness (scratch test); BRI=brittle index; UCS= uniaxial compressive strength; c'=cohesion; ϕ'=friction angle; DV=deviatoric stress in TXT.

Finally, a way to obtain reliable scenarios with numerical simulations of the effect of CO2 injection in reservoir rocks is to set up sensitivity analyses within a reasonable range of rock properties. The modeling results should be evaluated in terms of the effects of variability in each of the input parameters on the output ones and in the framework of site evidences in similar conditions.

2.1 Conclusion

This WP addressed the effect of gas injection on the mechanical response of sedimentary rocks.

The study showed that a large database of laboratory geomechanical tests carried out with CO2 injection is available, while N2 injection is marginally investigated and H2 injection into sedimentary rocks is currently under development. The gas N2 is used for the determination of the porosity of the rocks or as a control gas (Fuchs et al., 2019). Consequently, the exposure of rocks to N2 is expected to have negligible effects, in agreement with the experiments of Hu et al. (2019) described in the previous paragraphs.

The conclusions of the thorough reviews of CO2- fluid-rock interactions presented by Rohmer et al. (2016) and Peter et al. (2022) and considerations of Huang et al. (2020) on the same subject suggest that the role of injection of CO2 on rocks can be divided into two categories:

- the influence of CO2 on the mechanical parameters of rock is negligible
- the CO2 degrades the mechanical parameters of the rock which was mainly due to the mineral dissolution, pore size distribution modification induced by the presence of CO2

These conclusions are undoubtedly reasonable and are corroborated by a discrete number of experimental feedbacks.

However, the detailed analysis of some experimental studies reported in this WP have evidenced that there are still several uncertainties on the results.

The dissolution and precipitation of minerals due to CO2-acidified brine injection could decrease or increase the strength and stiffness of the rock, depending on the particular material and its composing mineral, even in the same rock.

The exposure of rocks to CO2-rich brines under various salinity content, temperatures and pressures have resulted in mixed conclusions regarding effects on stiffness and strength of the rock.

The occurrence of wide data scattering in the analyzed geomechanical tests can be attributed to the rock damage before testing, induced by the process of coring and specimen preparation and/or lithological varieties of the rock texture, pore space distribution and mineralogical composition within the sample. All these effects make difficult the comparison of lab tests.

Kim & Makhnenko (2022) argued that most existing studies still show significant inconsistencies that highly depend on the loading path, material, and testing conditions. They highlight the importance of adequately characterizing the rock.

Given that the geomechanical input parameters are never known precisely, because of the variability of rock, it is necessary to evaluate the type of uncertainties. Some uncertainties involved in these parameters are intrinsic and others are due to lack of knowledge or understanding of these parameters.

The variability in the results indicates that more (experimental) data are needed to cover the evidenced uncertainties, reported in this WP.

The main outcome of this analysis is that the geomechanical lab tests should be carried out with standard or at least similar procedures, in order to make easier the comparison of the results. Furthermore, a more rigorous description of the test methods and related results could help in the evaluation of the rock response when exposed to CO2.

3 Advances of research on H2 storage

Finally, a brief summary on the advances of research on H2 storage is reported in the following.

The most recent review on H2 injection and withdrawal is presented by Corina et al. (2022). This review describes the advances in research and the available experimental data. In this report are not

noticed geomechanical tests on rock flooded with H2. There are some references related to the CO2 effect on rock behavior that can be extended to H2.

Hydrogen injected into a porous reservoir will change the chemical equilibrium between the formation pore water, dissolved gases and the rock matrix. Resulting geochemical reactions could lead to:

1. significant loss of hydrogen;
2. contamination of the stored hydrogen by the production of other gases (e.g. H2S);
3. mineral dissolution/precipitation leading to enhanced or reduced injectivity;
4. mineral dissolution leading to opening of migration pathways through the caprock;
5. mineral dissolution impacting the mechanical properties of the reservoir and the caprock.

Interactions between hydrogen, fluids and rocks result in a variety of mineralogic reactions depending on the rock and fluid composition.

The transformations triggered by the pore fluid pH variations, such as carbonate and sulphate dissolution at low pH and stress corrosion microcracking in quartz and feldspar at high pH, are the most significant in term of alteration of the rock mechanical properties (Schimmel et al., 2019, 2021).

Heinemann et al. (2021) argue that repetitive injection of dry hydrogen could lead to the pervasive drying out of the reservoir, changing the mechanical properties over time. The direct consequences would be the progressive diminution of fluid rock reactions threatening the reservoir integrity, but the drying of clays would induce their shrinkage and may reverse the self-sealing properties of fractures leading to the reopening of leakage pathways (Song and Zhang, 2013).

Schimmel et al. (2021) have performed cyclic compaction experiments on quartz aggregates at various pH conditions and shown that total permanent deformation is mostly acquired during the first cycles.

Indeed, the cumulated grain cracking and grain reorientation during the compaction increase the surface contact between grains, which reduces the intergranular stress. Thus, crack growth and grain failure may progressively be impeded. When scaled to a UHS porous reservoir, hydrogen injection could trigger a response of the reservoir involving dissolution of carbonates and sulphate as well as grain crushing and local compaction

These processes will alter porosity and mechanical and flow properties of the reservoir.

The response will be time-dependent, i.e. pH equilibration to higher values could trigger even more compaction and stiffening of the reservoir, but this effect likely will stabilize after a few cycles.
In this scenario, the poroelastic response of the reservoir will be highly dependent on the chemical environment in the early stages of operations and becomes more stable and predictable in later stages.

References

Alam, M. M., Hjuler, M. L., Christensen, H. F., & Fabricius, I. L. (2014). Petrophysical and rock-mechanics effects of CO2 injection for enhanced oil recovery: Experimental study on chalk from South Arne field, North Sea. *Journal of Petroleum Science and Engineering*, *122*, 468-487.

Aman, M., Espinoza, D. N., Ilgen, A. G., Major, J. R., Eichhubl, P., & Dewers, T. A. (2018). CO2-induced chemo-mechanical alteration in reservoir rocks assessed via batch reaction experiments and scratch testing. *Greenhouse Gases: Science and Technology*, *8*(1), 133-149.

André, L., Audigane, P., Azaroual, M., & Menjoz, A. (2007). Numerical modeling of fluid–rock chemical interactions at the supercritical CO2–liquid interface during CO2 injection into a carbonate reservoir, the Dogger aquifer (Paris Basin, France). *Energy conversion and management*, *48*(6), 1782-1797.

Bemer, E., & Lombard, J. M. (2010). From injectivity to integrity studies of CO2 geological storage-chemical alteration effects on carbonates petrophysical and geomechanical properties. *Oil & Gas Science and Technology–Revue de l'Institut Français du Pétrole*, *65*(3), 445-459.

Bolourinejad, P. (2015). Effects of impurities on subsurface CO2 storage in gas fields in the northeast Netherlands (Doctoral dissertation, University of Groningen).

Bolourinejad, P., & Herber, R. (2015). Chemical effects of sulfur dioxide co-injection with carbon dioxide on the reservoir and caprock mineralogy and permeability in depleted gas fields. *Applied Geochemistry*, *59*, 11-22.

Corina, A., Zikovic, V., Soustelle, V. & Ter Heege, J. 2022: Review of current practices and existing experimental data for well and rock materials under cyclic hydrogen injection and withdrawal, H2020 HyUSPRe project report.

Erickson, K. P., Lempp, C., & Pöllmann, H. (2015). Geochemical and geomechanical effects of scCO2 and associated impurities on physical and petrophysical properties of Permotriassic Sandstones (Germany): an experimental approach. *Environmental Earth Sciences*, *74*(6), 4719-4743.

Espinoza, D. N., & Santamarina, J. C. (2012). Clay interaction with liquid and supercritical CO2: The relevance of electrical and capillary forces. *International Journal of Greenhouse Gas Control*, *10*, 351-362.

Espinoza, D. N., Jung, H., Major, J. R., Sun, Z., Ramos, M. J., Eichhubl, P., ... & Dewers, T. A. (2018). CO2 charged brines changed rock strength and stiffness at Crystal Geyser, Utah: Implications for leaking subsurface CO2 storage reservoirs. *International Journal of Greenhouse Gas Control*, *73*, 16-28.

Foroutan, M., Ghazanfari, E., Amirlatifi, A., & Perdrial, N. (2021). Variation of pore-network, mechanical and hydrological characteristics of sandstone specimens through CO2-enriched brine injection. *Geomechanics for Energy and the Environment*, *26*, 100217.

Fuchs, S. J., Espinoza, D. N., Lopano, C. L., Akono, A. T., & Werth, C. J. (2019). Geochemical and geomechanical alteration of siliciclastic reservoir rock by supercritical CO2-saturated brine formed during geological carbon sequestration. *International Journal of Greenhouse Gas Control*, *88*, 251-260.

Ganzer, L., Reitenbach, V., Pudlo, D., Albrecht, D., Singhe, A. T., Awemo, K. N., ... & Gaupp, R. (2014). Experimental and numerical investigations on CO2 injection and enhanced gas recovery effects in Altmark gas field (Central Germany). *Acta Geotechnica*, *9*(1), 39-47.

Gaus, I. (2010). Role and impact of CO2–rock interactions during CO2 storage in sedimentary rocks. *International journal of greenhouse gas control*, *4*(1), 73-89.

Grgic, D. (2011). Influence of CO2 on the long-term chemomechanical behavior of an oolitic limestone. *Journal of Geophysical Research: Solid Earth*, *116*(B7).

Grombacher, D., Vanorio, T., & Ebert, Y. (2012). Time-lapse acoustic, transport, and NMR measurements to characterize microstructural changes of carbonate rocks during injection of CO 2-rich water. *Geophysics*, *77*(3), WA169-WA179.

Gunter, W. D., Perkins, E. H., & Hutcheon, I. (2000). Aquifer disposal of acid gases: modelling of water–rock reactions for trapping of acid wastes. *Applied geochemistry*, *15*(8), 1085-1095

Hangx, S. J., Spiers, C. J., & Peach, C. J. (2010). Mechanical behavior of anhydrite caprock and implications for CO2 sealing capacity. Journal of Geophysical Research: Solid Earth, 115(B7)

Hangx, S., van der Linden, A., Marcelis, F., & Bauer, A. (2013). The effect of CO2 on the mechanical properties of the Captain Sandstone: Geological storage of CO2 at the Goldeneye field (UK). *International Journal of Greenhouse Gas Control*, *19*, 609-619.

Harbert, W., Goodman, A., Spaulding, R., Haljasmaa, I., Crandall, D., Sanguinito, S., ... & Frailey, S. (2020). CO2 induced changes in Mount Simon sandstone: Understanding links to post CO2 injection monitoring, seismicity, and reservoir integrity. *International Journal of Greenhouse Gas Control*, *100*, 103109.

Heinemann, N., J. Alcalde, J.M. Miocic, S.J.T. Hangx, J. Kallmeyer, C. Ostertag-Henning, A. Hassanpouryouzband, E.M. Thaysen, G.J. Strobel, C. Schmidt-Hattenberger, K. Edlmann, M. Wilkinson, M. Bentham, R. Stuart Haszeldine, R. Carbonell & A. Rudloff, 2021. Enabling large-scale hydrogen storage in porous media – the scientific challenges. *Energy & Environmental Science*, 14(2), 853-64.

Hu, S., Li, X., Bai, B., Shi, L., Liu, M., & Wu, H. (2017). A modified true triaxial apparatus for measuring mechanical properties of sandstone coupled with CO2-H2O biphase fluid. *Greenhouse Gases: Science and Technology*, *7*(1), 78-91.

Ilgen, A. G., Newell, P., Hueckel, T., Espinoza, D. N., & Hu, M. (2019). Coupled chemical-mechanical processes associated with the injection of CO2 into subsurface. In *Science of carbon storage in deep saline formations* (pp. 337-359). Elsevier.

Kampman, N., Bickle, M., Wigley, M., & Dubacq, B. (2014). Fluid flow and CO2–fluid–mineral interactions during CO2-storage in sedimentary basins. Chemical Geology, 369, 22-50

Kaszuba, J. P., Janecky, D. R., & Snow, M. G. (2005). Experimental evaluation of mixed fluid reactions between supercritical carbon dioxide and NaCl brine: Relevance to the integrity of a geologic carbon repository. *Chemical Geology*, *217*(3-4), 277-293.

Kim, K., & Makhnenko, R. Y. (2022). Short-and Long-Term Responses of Reservoir Rock Induced by CO2 Injection. *Rock Mechanics and Rock Engineering*, 1-21.

Kim, K., Vilarrasa, V., & Makhnenko, R. Y. (2018). CO2 injection effect on geomechanical and flow properties of calcite-rich reservoirs. *Fluids*, *3*(3), 66.

Lei, X., & Xue, Z. (2009). Ultrasonic velocity and attenuation during CO2 injection into water-saturated porous sandstone: Measurements using difference seismic tomography. *Physics of the Earth and Planetary Interiors*, *176*(3-4), 224-234.

Liteanu, E., Spiers, C. J., & De Bresser, J. H. P. (2013). The influence of water and supercritical CO2 on the failure behavior of chalk. *Tectonophysics*, *599*, 157-169

Marbler, H., Erickson, K. P., Schmidt, M., Lempp, C., & Pöllmann, H. (2013). Geomechanical and geochemical effects on sandstones caused by the reaction with supercritical CO2: an experimental approach to in situ conditions in deep geological reservoirs. Environmental earth sciences, 69(6), 1981-1998.

Matter, J. M., Stute, M., Snæbjörnsdottir, S. Ó., Oelkers, E. H., Gislason, S. R., Aradottir, E. S., ... & Broecker, W. S. (2016). Rapid carbon mineralization for permanent disposal of anthropogenic carbon dioxide emissions. *Science*, *352*(6291), 1312-1314.

McGrail, B. P., Schaef, H. T., Glezakou, V. A., Dang, L. X., & Owen, A. T. (2009). Water reactivity in the liquid and supercritical CO2 phase: Has half the story been neglected?. *Energy Procedia*, *1*(1), 3415-3419.

Mikhaltsevitch, V., Lebedev, M., & Gurevich, B. (2014). Measurements of the elastic and anelastic properties of sandstone flooded with supercritical CO2. *Geophysical Prospecting*, *62*(6), 1266-1277.

Miller, Q. R., Wang, X., Kaszuba, J. P., Mouzakis, K. M., Navarre-Sitchler, A. K., Alvarado, V., ... & Heath, J. E. (2016). Experimental study of porosity changes in shale caprocks exposed to carbon dioxide-saturated brine II: Insights from aqueous geochemistry. *Environmental engineering science*, *33*(10), 736-744.

Mouzakis, K. M., Navarre-Sitchler, A. K., Rother, G., Bañuelos, J. L., Wang, X., Kaszuba, J. P., ... & McCray, J. E. (2016). Experimental study of porosity changes in shale caprocks exposed to CO2-saturated brines I: Evolution of mineralogy, pore connectivity, pore size distribution, and surface area. *Environmental engineering science*, *33*(10), 725-735.

Ojala, I. O. (2011). The effect of CO2 on the mechanical properties of reservoir and cap rock. *Energy Procedia*, *4*, 5392-5397.

Peter, A., Yang, D., Eshiet, K. I. I. I., & Sheng, Y. (2022). A Review of the Studies on CO2–Brine–Rock Interaction in Geological Storage Process. *Geosciences*, *12*(4), 168.

Pudlo, D., Reitenbach, V., Albrecht, D., Ganzer, L., Gernert, U., Wienand, J., ... & Gaupp, R. (2012). The impact of diagenetic fluid–rock reactions on Rotliegend sandstone composition and petrophysical properties (Altmark area, central Germany). Environmental Earth Sciences, 67(2), 369-384.

Rathnaweera, T. D., Ranjith, P. G., Perera, M. S. A., Haque, A., Lashin, A., Al Arifi, N., ... & Yasar, E. (2015). CO2-induced mechanical behaviour of Hawkesbury sandstone in the Gosford basin: An experimental study. *Materials Science and Engineering: A*, *641*, 123-137.

Rimmelé, G., Barlet-Gouédard, V., & Renard, F. (2010). Evolution of the petrophysical and mineralogical properties of two reservoir rocks under thermodynamic conditions relevant for CO2 geological storage at 3 km depth. Oil & Gas Science and Technology–Revue de l'Institut Français du Pétrole, 65(4), 565-580.

Rohmer, J., Pluymakers, A., & Renard, F. (2016). Mechano-chemical interactions in sedimentary rocks in the context of CO2 storage: Weak acid, weak effects?. *Earth-Science Reviews*, *157*, 86-110.

Rutqvist, J. (2012). The geomechanics of CO2 storage in deep sedimentary formations. Geotechnical and Geological Engineering, 30(3), 525-551.

Schimmel, M.T.W., S.J.T. Hangx & C.J. Spiers, 2019. Impact of Chemical Environment on Compaction Creep of Quartz Sand and Possible Geomechanical Applications. *Journal of Geophysical Research: Solid Earth*, 124(6), 5584-606.

Schimmel, M.T.W., S.J.T. Hangx & C.J. Spiers, 2021. Impact of Chemical Environment on Compaction Behaviour of Quartz Sands during Stress-Cycling. *Rock Mechanics and Rock Engineering*, 54(3), 981-1003

Shi, Z., Sun, L., Haljasmaa, I., Harbert, W., Sanguinito, S., Tkach, M., ... & Jessen, K. (2019). Impact of Brine/CO2 exposure on the transport and mechanical properties of the Mt Simon sandstone. *Journal of Petroleum Science and Engineering*, *177*, 295-305.

Tarokh, A., Makhnenko, R. Y., Kim, K., Zhu, X., Popovics, J. S., Segvic, B., & Sweet, D. E. (2020). Influence of CO2 injection on the poromechanical response of Berea sandstone. *International Journal of Greenhouse Gas Control*, *95*, 102959.

Vanorio, T., Nur, A., & Ebert, Y. (2011). Rock physics analysis and time-lapse rock imaging of geochemical effects due to the injection of CO 2 into reservoir rocks. *Geophysics*, *76*(5), O23-O33.
Vialle, S., & Vanorio, T. (2011). Laboratory measurements of elastic properties of carbonate rocks during injection of reactive CO2-saturated water. *Geophysical Research Letters*, *38*(1).

Xu, T., Apps, J. A., Pruess, K., & Yamamoto, H. (2007). Numerical modeling of injection and mineral trapping of CO2 with H2S and SO2 in a sandstone formation. *Chemical Geology*, *242*(3-4), 319-346.

Yoksoulian, L. E., Freiburg, J. T., Butler, S. K., Berger, P. M., & Roy, W. R. (2013). Mineralogical alterations during laboratory-scale carbon sequestration experiments for the Illinois Basin. *Energy Procedia*, *37*, 5601-5611